

**Electronics and Communications Engineering Department** 

### **Design of Wide Band RF Power Amplifier**

A Thesis
Submitted in partial fulfillment for the requirements of the degree of **Master of Science in Electrical Engineering** 

Submitted by

#### Mohammed Ezzat Yassin Abd El-Galil Esmail

Electronics and Communications Eng. Dept. Faculty of Engineering - Ain Shams University

Supervised by

#### Prof. Dr. Esmat Abdel-Fattah Abdallah

Professor - Microstrip Department Electronics Research Institute

#### **Prof. Dr. Hadia Mohamed El-Hennawy**

Professor - Faculty of Engineering Ain Shams University

#### Dr. Hany Mohamed Taher

Researcher - Microstrip Department Electronics Research Institute



#### **Examiners Committee**

Name: Mohammed Ezzat Yassin Abd El-Galil Esmail Thesis: Design of Wide Band RF Power amplifier Degree: Master of Science in Electrical Engineering (Electronics and Communications **Engineering**) Title, Name and Affiliation Signature 1. Prof. Dr. Ibrahim Ahmed Salem Former Director – Military Technical College 2. Prof. Dr. Ibrahim Ahmed Salem . . . . . . . . . . . . . . . . Electronics and Communications Eng. Dept. Faculty of Engineering - Ain Shams University 3. Prof. Dr. Esmat Abdel-Fattah Abdallah . . . . . . . . . . . . . . . . Microstrip Department, **Electronics Research Institute** 4. Prof. Dr. Hadia Mohamed El-Hennawy Electronics and Communications Eng. Dept. Faculty of Engineering - Ain Shams University

Date: / /2012

#### **STATEMENT**

This Thesis is submitted to Ain Shams University in partial fulfillment of the degree of Master of Science in Electrical Engineering.

The work included in this thesis was carried out by the author in the Department of Electronics and Communications Engineering, Ain Shams University.

No part of this Thesis has been submitted for a degree or a qualification at any other university or institute.

Name	: Mohammed Ezzat Yassin Abd El-Galil Esmail	

Signature:

Date :

### Acknowledgment

### All my thanks to Allah, to the successful completion of this work.

I express my deepest gratitude and thanks to Prof. Dr. Esmat A. Abdallah, Former President of Electronics Research Institute, Electronics Research Institute, for her continuous supervision support. Prof.Esmat is behind all analytical, technical and even spiritual actions throughout this work. Without her encouragement, the thesis could not reach this level.

Thanks are also due to Prof. Hadia El Hennawi, Former Dean of the Faculty of Engineering, Ain Shams University, for her understanding, patience, encouragement, besides, overcoming any obstacles that might interfere with my work.

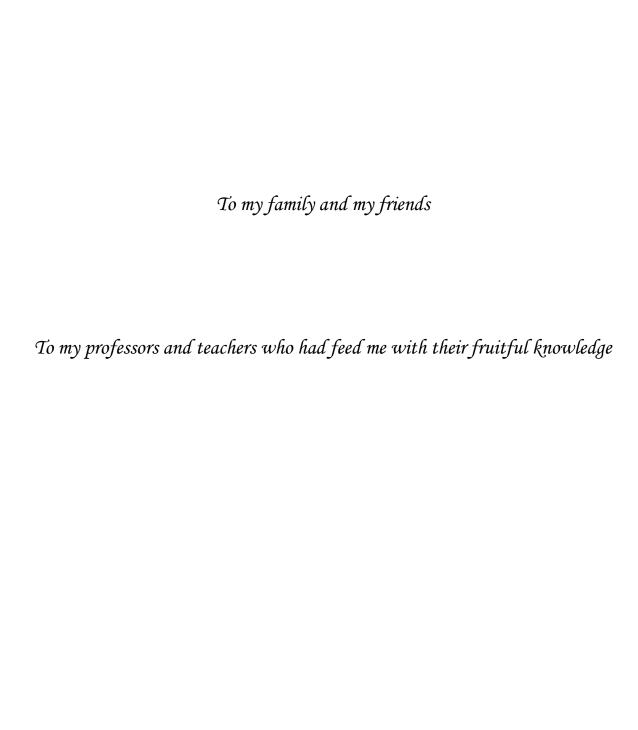
Also, my deepest gratitude and sincerest thanks to Dr. Hany M. Taher for his supervision.

My deepest gratitude and sincerest thanks to Dr. Ahmed S. Mahmoud for his fruitful guidance through the course of the work, encouragement, endless help especially in fabrication and measurements and many illuminating discussions.

Thanks for my colleagues and friends in Microstrip Department and the Electronics Research Institute staff for being around me helping and caring.

Many thanks for my mother, father and brothers for their great hearts which looked after me all these years.

To my mother and my father, who had a great influence on shaping my character



### **ABSTRACT**

The power amplifier is the most critical element in the transmitter path because it is the most power hungry block and also affects the total performance of the system. The purpose of power amplifier is to amplify the power of the RF signal before it is fed to the antenna. It is expected to provide a sufficient output power for reliable transmission. High gain reduces the number of amplifier stages required to deliver the desired output power and hence reduces the size and manufacturing cost. High efficiency improves thermal management, better lifetime and operational costs. Good linearity is necessary for bandwidth efficient modulation. However, these are contrasting requirements and a typical power amplifier design would require a certain level of compromise. There are several types of power amplifiers which differ from each other in terms of gain, linearity, output power or efficiency depending on the application in which the communication system is used.

In contrast to the standard GSM, the UMTS standard allows mobile and wireless transmission of broadband signals, e.g. video and internet data. The UMTS standard offers high voice quality, high data rates and high network capacity and thus, accelerates the consolidation of the communication, information and mobile multimedia technology. Despite the roll-out of the UMTS standard, GSM is still an important part of the mobile communication and will remain for some years. UMTS mobile phones are conceived in such a way that they also work in a GSM network (dual mode) and therefore, data transfer is also guaranteed in the areas, similarly multi-standard transceiver base stations which support the UMTS-standard and the GSM-standard are in demand.

The challenge of this thesis is to design a power amplifier with 2 GHz center frequency which is able to operate in the UMTS-frequency band (center frequency around 2.14 GHz) and also in the frequency bands of GSM-1800 (center frequency around 1.8 GHz). This so-called multiband base station concept is also able to handle the variation of the used frequency bands in different global regions. The flexibility of the operating frequency offered by this amplifier concept enables short reaction time for newly-introduced standards.

The thesis introduces the design, simulation and manufacturing of class A power amplifier. The first contribution is designing and realizing 2 GHz high linearity wide band class A power amplifier which serves as a stage in multiple stages power amplifier for UMTS and GSM standards. A ready-

made software package advanced design system (ADS) is used in the design and optimization process of the power amplifier. The measurements results of the power amplifier with 3-dB bandwidth extended from 1.5 to 2.3 GHz are 31.242 dBm output power, 17 dB gain, 30% efficiency, 0.8 dB/dB maximum deviation AM/AM and 0.5 degree/dB maximum deviation AM/PM conversions. The second achievement is implementing a DGS filter at the amplifier output for total elimination of the unwanted harmonics. A ready-made software package Zeland IE3D is used in the design and optimization process of the filters. The DGS filter used is constructed by three units array of the Square head dumbbell shape to be suitable for covering the required stop band from 4 to 10 GHz. The dielectric material used is Teflon with permittivity of 2.33 and dielectric thickness of 0.508 mm. The performance of the DGS microstrip line offers -41.2, -45.6, -56.8 and -41 dB attenuation for the second, third, fourth and fifth harmonic components, respectively, which is sufficient to force the harmonic components beyond -60 dBc. The total system performance which consists of the class A power amplifier followed by the DGS filter at the output has measured results of 31.135 dBm output power, 16.9 dB power gain while the harmonics were almost totally removed.

## **Table of contents**

Statement	Page I
Acknowledgement	II
Abstract	IV
Table of Contents	VI
Lists of Figures	IX
List of Tables	XIII
List of Symbols	XIV
List of Abbreviations	XV
Chapter 1: Introduction	
1.1. Overview	1
1.2. Main objective of the thesis	2
1.3. Achievements	2 2 3
1.4. Thesis organization	3
Chapter 2: RF power amplifier	
2.1. Introduction	4
2.2. Power amplifier in communication system	4
2.3. Amplifier parameters	5
2.3.1. Amplifier gain	5
2.3.2. Stability	6
2.3.3. Efficiency	8
2.3.4. Noise	9
2.3.5. Linearity	10
2.3.5.1. 1 dB compression point	10
2.3.5.2. Inter-modulation distortion	11
2.3.5.3. Third order intercept point	11
2.3.5.4. Phase distortion	12
2.3.5.5. Adjacent channel power ratio	13
2.4. Power amplifier classifications	14
2.4.1. Linear amplifiers	15
2.4.1.1. Class A	15
2.4.1.2. Class B	16
2.4.1.3. Class AB 2.4.1.4. Class C	17 18
2.4.1.4. Class C 2.4.2. Switching amplifiers	19
2.5. Impedance matching	20
2.5.1. Matching using lumped elements	20
2.5.1.1. Design for maximum available gain	21
2.5.1.2. Matching for a specified gain	23
2.5.1.3. Matching for optimum noise figure	24
2.5.2. Matching using distributed elements	25
2.5.2.1. Richard's transformation	25
2.5.2.2. Kuroda's identities	26

#### **Chapter 3: Defected Ground Structures (DGS)** 3.1. Introduction 28 3.2. DGS unit 28 29 3.2.1. Influence of the square lattice dimension 3.2.2. Influence of the gap width 30 3.3. Equivalent circuits of DGS 30 3.3.1. Parallel LC-circuit 31 32 3.3.2. Parallel RLC-circuit 33 3.3.3. $\pi$ -equivalent circuit 3.4. Periodic DGS 35 35 3.4.1. Single, double and triple DGS patterns 3.4.2. Influence with head separation 36 3.5. Various DGS structures 37 3.5.1. Rectangular DGS 37 3.5.2. Circular head DGS 38 3.5.3. Arrow-head DGS 39 3.6. Application of DGS in power amplifier 40 3.6.1. Harmonic suppression 40 3.6.2. Size reduction 43 3.6.3. Using $\frac{\lambda}{4}$ bias line combined with DGS 46 **Chapter 4: Design and simulation** 48 4.1. Class A power amplifier 4.1.1. Device under simulation 48 4.1.2. DC analysis 49 4.1.3. Small-signal(S-parameter) simulations 52 4.1.4. Design of matching network (IMN, OMN) 53 4.1.4.1. Load pull simulation 53 4.1.4.2. Output and input matching networks 54 4.1.5. ADS schematic simulation and optimizations 56 4.1.5.1. First design 56 4.1.5.2. Optimized design 63 4.1.6. ADS momentum simulation and optimization 68 4.1.6.1. First layout 68 4.1.6.2. Optimized layout 73 4.2. Microstrip line using DGS 79 4.2.1 Introduction 79 4.2.2 Seven Poles LPF with DGS 79 4.2.2.1 Chebyshev LPF design using DGS 80 4.2.2.2 Square head dumbbell shaped DGS resonator 81 82 4.2.2.3 LPF design method 4.2.2.4 LPF design 83 4.3. Power amplifier with the DGS filter simulation 88 90 **Chapter 5: Fabrication and measurements**

5.1. Power amplifier measurements	90
5.1.1. Introduction	90
5.1.2. S-parameters measurement	91
5.1.3 Power measurements	92
5.1.4 Linearity measurements	94
5.2. DGS filter measurements	96
5.3. total system measurements	
Chapter 6: Conclusions and Suggestions for Future Work	99
6.1 Introduction	99
6.2 Conclusion	99
6.3 Suggestions for Future Work	100
Appendix (A)	101
List of reference	105

# **List of Figures**

		Page
Fig. 2.1	Wireless communication block diagram	4
Fig. 2.2	Two-port network with voltage source at its input and a load terminating the	6
	output port.	
Fig. 2.3	Regions of stabilities for input stability regions as: (a) $ S_{11}  > 1$ and (b)	7
	$ S_{11}  < 1$	
Eig 2.4		8
Fig. 2.4	Regions of stabilities for output stability circle as: (a) $ S_{11}  > 1$ and (b) $ S_{11}  < 1$	
Fig. 2.5	1- dB compression characteristics	10
Fig. 2.6	Frequency spectrum of a two-tone signal	11
Fig. 2.7	Third order intercept point	12
Fig. 2.8	(a) AM-AM conversion, (b) AM-PM conversion, and (c) combination of	13
	AM-AM and AM-PM conversions	
Fig. 2.9	Plot of adjacent power channel	14
Fig. 2.10	Basic PA topology	15
Fig. 2.11	Q-point of Class-A, AB, B and C type amplifiers	15
Fig. 2.12	Conduction angle of class A	16
Fig. 2.13	Conduction angle of class B	17
Fig. 2.14	Conduction angle of class AB	18
Fig. 2.15	Conduction angle of class C	18
Fig. 2.16	Block diagram of an amplifier	20
Fig. 2.17	Using smith chart to determine lumped elements for matching	22
Fig. 2.18	Matching for specified gain	24
Fig. 2.19	Richard's transformation	26
Fig. 2.20	The four Kuroda's identities where $n^2 = 1 + Z_2/Z_1$	27
Fig. 3.1	The first DGS unit	29
Fig. 3.2	Simulated S-parameters for the proposed DGS unit lattices. The gap distance	29
	g equal to 0.637 mm which is kept constant for all cases	
Fig. 3.3	Simulated S-parameters for the DGS unit lattices. The lattice dimension is	30
	kept constant for all cases	
Fig. 3.4	Conventional design and analysis method of dumbbell DGS	31
Fig. 3.5	LC equivalent circuit: (a) equivalent circuit of the dumbbell DGS circuit and	32
	(b) Butterworth-type one-pole prototype low-pass filter circuit	
Fig. 3.6	The equivalent circuit of the DGS with parallel resistance	33
Fig. 3.7	The $\pi$ -equivalent circuit of the dumbbell DGS	34
Fig. 3.8	Periodic DGS: (a) HPDGS and (b) VPDGS	35
Fig. 3.9	Simulation results of single, double and triple DGS patterns	36
Fig. 3.10	Simulated S-parameters for different separation d	36
Fig. 3.11	Different DGS slots. These are rectangular, circular head, H-shape head and	37
	arrow-head defects (from left to right).	
Fig. 3.12	Simulated S-parameters for different length L and width g respectively	38
Fig. 3.13	Simulated S-parameters for different radius r and length L respectively	39

Fig. 3.14	Simulated S-parameters for different area A and length L respectively	40
Fig. 3.15	(a) The microstrip line with the proposed DGS and (b) The simulation results	42
Fig. 3.16	Class A power amplifier simulation results with and without using DGS, (a)	43
	Second harmonic, (b) Output power and (c) Power added efficiency	
Fig. 3.17	(a) Conventional microstrip line and (b) microstrip line with a unit DGS	44
Fig. 3.18	Electrical lengths (S <sub>21</sub> phases) of two microstrip lines: (a) Conventional	44
	microstrip line and (b) Microstrip line with a unit DGS	
Fig. 3.19	Simplified layout of the basic amplifier using: (a) conventional microstrip and (b) reduced microstrip using DGS	45
Fig. 3.20	Measured performance of: (a) Conventional amplifier and (b) Reduced length amplifier	46
Fig. 3.21	(a) Layout of a conventional microstrip line ( $w = 2.38$ , Unit = mm) and (b) layout of a 50 DGS micro strip line ( $a = 6$ , $b = 1$ , $g = 0.5$ and $c = w = 4.7$ )	47
Fig. 4.1	I-V curve simulations	50
Fig. 4.2	(a) The I-V curve and (b) Biasing point calculation	51
Fig. 4.3	The biasing network	51
Fig. 4.4	S-parameters simulation	52
Fig. 4.5	Load pull simulation	53
Fig. 4.6	Load pull analysis to determine load impedance for required output power and efficiency	54
Fig. 4.7	Smith Chart for the design of the output matching network	55
Fig. 4.8	Smith Chart for the design of the input matching network	56
Fig. 4.9	Build-up circuit	57
Fig. 4.10	Schematic of one tone harmonic balance simulation versus power sweeping	58
Fig. 4.11	One tone harmonic balance simulation versus power sweeping results	59
Fig. 4.12	The harmonic components of one tone harmonic balance simulation result:  (a) at 1-dB compression, and (b) at max. input	60
Fig. 4.13	Schematic of one tone harmonic balance simulation versus power sweeping	60
Fig. 4.14	One tone harmonic balance simulation versus frequency sweeping results	61
Fig. 4.15	Schematic of two tone harmonic balance simulation versus power sweeping	62
Fig. 4.16	Transducer power gain versus input power sweeping	62
Fig. 4.17	(a) The zoomed output spectrum showing 3_rd, 5_th and 7_th order IMD products and (b) Input and output third order intercept points	62
Fig. 4.18	Build-up circuit of the optimized design	64
Fig. 4.19	One tone harmonic balance simulation versus power sweeping results	65
Fig. 4.20	The harmonic components of one tone harmonic balance simulation result:  (a) at 1-dB compression and (b) at max. input	65
Fig. 4.21	One tone harmonic balance simulation versus frequency sweeping results:  (a) at 1-dB compression and (b) at max. input	66
Fig. 4.22	Transducer power gain versus input power sweeping	67
Fig. 4.23	(a) The zoomed output spectrum showing 3_rd, 5_th and 7_th order IMD products and (b) Input and output third order intercept points	67
Fig. 4.24	Amplifier layout	69
Fig. 4.25	One tone harmonic balance simulation versus power sweeping results	70

Fig. 4.26	The harmonic components of one tone harmonic balance simulation result:  (a) at 1-dB compression and (b) at max. input	71
Fig. 4.27	One tone harmonic balance simulation versus frequency sweeping results:  (a) at 1-dB compression and (b) at max. input	72
Fig. 4.28	Transducer power gain versus input power sweeping	73
Fig. 4.29	(a) The zoomed output spectrum showing 3_rd, 5_th and 7_th order IMD products and (b) Input and output third order intercept points	73
Fig. 4.30	The optimized layout	74
Fig. 4.31	One tone harmonic balance simulation versus power sweeping results	75
Fig. 4.32	The harmonic components of one tone harmonic balance simulation result:  (a) at 1-dB compression and (b) at max. input	76
Fig. 4.33	One tone harmonic balance simulation versus frequency sweeping results:  (a) at 1-dB compression and (b) at max. input	77
Fig. 4.34	Transducer power gain versus input power sweeping	78
Fig. 4.35	(a) The zoomed output spectrum showing 3_rd, 5_th and 7_th order IMD products and (b) Input and output third order intercept points	78
Fig. 4.36	Low-pass prototype filter with a ladder network structure (with odd number of reactive elements)	80
Fig. 4.37	Series inductor substitution	81
Fig.4.38	square-shape DGS resonator	82
Fig. 4.39	DGS cutoff and resonant frequency in dependence on DGS parameter $w_{50}/a$	82
Fig. 4.40	A 7th order low-pass prototype filter network structure	84
Fig. 4.41	LPF with DGS—equivalent circuit	85
Fig. 4.42	Structure of proposed filter	87
Fig. 4.43	S-parameters of EM simulation	87
Fig. 4.44	The fundamental output power and harmonics simulation results of : (a) the power amplifier without the DGS filter, and (b) the power amplifier with the DGS filter.	89
Fig. 5.1	Power amplifier layout.	90
Fig. 5.2	The fabricated power amplifier.	91
Fig. 5.3	Setup for the S-parameters measurement.	91
Fig. 5.4	The simulation and measurement results of: (a) $S_{11}$ , and (b) $S_{22}$ .	91
Fig. 5.5	The simulation and measurement results of $S_{21}$ .	92
Fig. 5.6	Power measurements setup.	92
Fig. 5.7	The simulated and measured results of: (a) output power, (b) power added efficiency, and (c) power gain.	93
Fig. 5.8	The simulation and measurement results of the power gain versus frequency sweeping.	94
Fig. 5.9	Linearity measurements setup.	94
Fig. 5.10	ACPR measurement for WCDMA signals.	95
Fig. 5.11	The AM-AM and AM-PM measurement results.	96
Fig. 5.12	The fabricated DGS filter: (a) top view, and (b) bottom view.	96
Fig. 5.13	Simulation and measurement results of the DGS filter.	97

## **List of Tables**

		Page
Table 1.1	Power amplifier specifications for GSM and UTMS standards	2
Table 2.1	Summary of power amplifier classes	20
Table 4.1	Typical EFA480C-180F properties	49
Table 4.2	S-parameters and stability results	52
Table 4.4	Prototype filter elements and ideal circuit elements	84
Table 4.4	Final Filter Parameters	86

# **List of Symbols**

$A_{V}$	Voltage gain
A <sub>V<sub>loaded</sub></sub>	Loaded voltage gain
С	Capacitance
F	Actual noise figure
f	Frequency
G	Power gain
$G_{T}$	Transducer gain
h	Dielectric thickness
K	Stability factor
L	Inductance
P <sub>avail</sub>	Power available from the source
P <sub>load</sub>	Power delivered to the load
$R_{L}$	Load resistance
t	Strip thickness
$Z_0$	Characteristic impedance
Γ	Reflection coefficient
$\epsilon_{ m r}$	Dielectric constant
η	Efficiency
θ	Electrical length
λ	Wavelength